

Perspective

Do Pegmatites Crystallise Fast? A Perspective from Petrologically-Constrained Isotopic Dating

Daniil V. Popov 

French National Centre for Scientific Research (CNRS), Université d'Orléans, CEMHTI UPR 3079, 45071 Orléans, France; daniil.popov@cnrs-orleans.fr or d.vs.popov@gmail.com

Abstract: Most recent studies consider the formation of individual pegmatite bodies to be a fast process with estimated crystal growth rates reaching a whopping 10 m/day. This opinion is presumably underpinned by the traditional way of thinking of them as the end products of magmatic fractionation. Indeed, modelling has shown that if a pegmatite-forming substance with a temperature near granitic solidus intrudes into a much colder host rock, as recorded in some outcrops, it must cool rapidly. From here, a conclusion is made that the crystallisation must likewise be rapid. However, this view is challenged by several studies that published isotopic dates supported by petrological characterisation of the analysed materials, which suggested or can be used to suggest that some minerals in pegmatites grew over millions of years. Surprisingly, such in-depth work on the geochronology of individual pegmatite bodies is relatively uncommon, so it is early to make generalisations. Here, I highlight some of the existing evidence with the aim to stimulate further research into the timescales of pegmatite crystallisation, including the use of petrologically constrained isotopic dating.

Keywords: pegmatite; rate of crystallisation; geochronology



Citation: Popov, D.V. Do Pegmatites Crystallise Fast? A Perspective from Petrologically-Constrained Isotopic Dating. *Geosciences* **2023**, *13*, 297. <https://doi.org/10.3390/geosciences13100297>

Academic Editor: Jesus Martinez-Frias

Received: 7 July 2023

Revised: 21 August 2023

Accepted: 30 September 2023

Published: 2 October 2023



Copyright: © 2023 by the author. Licensee MDPI, Basel, Switzerland. This article is an open access article distributed under the terms and conditions of the Creative Commons Attribution (CC BY) license (<https://creativecommons.org/licenses/by/4.0/>).

1. Introduction

Pegmatites have long provoked fascination and curiosity in geoscientists, whether as rocks with unusual textures in general and gigantic crystals in particular [1]; as a source for many beautiful coloured stones [2], raw materials [3] and critical metals [4]; or as a petrological record of the transition from magmatic to hydrothermal crystallisation [5]. Although immense efforts have been made to understand how pegmatites form, there is no unanimity about this in the recent literature. Debated subjects include even such prime things as the physical nature of pegmatite-forming substances [1,6–8] and their relationship with large felsic intrusions [9–14]. All of these subjects, however, lie outside the scope of the present paper. Instead, I would like to draw readers' attention to the subject that has not really been a matter of debate in recent years, which is the timescales over which individual pegmatite bodies form.

Historically, pegmatites are regarded as the end product of the evolution of large felsic intrusions, within or near which many of them are found [1,6,7], even though a growing number of studies report pegmatites that lack spatial and temporal links to such bodies and thus could have formed by anatexis [9–14]. This historical framework of thinking leads to the idea that pegmatite-forming substances have starting temperatures near the granite solidus, and that their crystallisation rate is somehow related to the cooling rate of these substances after their emplacement into potentially much colder country rocks, which was estimated to reach 10^2 °C/week [15–17]. From here, it follows that isotopic dates of any primary mineral from pegmatites that did not leak radiogenic isotopes after its formation should be statistically equivalent. Consequently, most previous geochronological studies of pegmatites aimed to obtain a single number interpreted as the age of its complete crystallisation, while any scatter in the acquired dates was ascribed to some thermal disturbances or genetically unimportant alteration [9–14,18–29]. However, what if we

look at the results of isotopic dating of pegmatites without a priori constraints from our understanding of how they should form?

Relatively few previous studies of pegmatites present spatially resolved isotopic dates that are supplemented by detailed petrological characterisation of the analysed materials, and they often report significant scatter in the obtained apparent ages [24–33]. Some of these results were or can be taken as evidence for protracted, multi-stage and potentially polygenic origin of individual pegmatites, which challenges the very foundation of thinking of them as fast-forming products of the late-stage evolution of felsic magmas. Here, I review four examples that seem most interesting to me with the aim to highlight that geochronological tools can be used to investigate the timescales of pegmatite crystallisation and thereby stimulate further efforts in this direction. While it is too early to make generalisations at this stage, I believe that having more comparable evidence at hand will advance our understanding of how pegmatites form.

2. Examples of Protracted (Re)Crystallisation in Pegmatites

The term ‘pegmatite’ has been used to describe rocks of highly variable but broadly igneous chemical and mineral composition, at least some portions of which consist of very large cm to m scale crystals [15]. Here, I simply inherit its use from the reviewed articles, which may of course obscure some important petrological and genetic differences between the rocks and the processes in their focus. I believe that this is justifiable in context of the present contribution because it seeks to highlight that geochronological evidence may be one of the keys to reveal such differences and understand their causes. Petrological studies of pegmatites typically identify a logically continuous sequence of events that are considered as part of some pegmatite-forming process, such as crystallisation from melt followed by precipitation from fluid that exsolved from it, and may further distinguish one or several later discontinuous events that are regarded as genetically unrelated overprint, such as weathering [34–36]. My paper is only concerned with evidence relating to the first type of events, that is, with geochronological data from minerals that were traditionally considered to have formed at some stage of a continuous pegmatite-forming process, whatever it might be.

I have selected four studies from different localities that demonstrate that any stage of mineral growth in pegmatites can be protracted. These cover a clearly early phase in the crystallisation sequence, which is zircon from the Finero pegmatites; a gemstone, albeit atypical, which is alkali feldspar from the Itrongay pegmatites; a potential ore mineral, which is Li-rich mica from the Pakeagama Lake pegmatite; and what was initially assumed to be a product of autometasomatism, which is a muscovite and buddingtonite-bearing pseudomorph after beryl from the Volyn pegmatites. I use the following abbreviations in the text and figures below: CL—cathodoluminescence; BSEs—back-scattered electrons; LA-ICP-MS—laser ablation inductively coupled plasma mass spectrometry; TIMS—thermal ionisation mass spectrometry; CGMs—columbite group minerals; Ms—muscovite; Lpd—lepidolite and F-, Rb-, Cs- and Li-rich zones in muscovite; bud—buddingtonite; tob—tobelite.

2.1. Finero Pegmatites

Schaltegger et al. [30] studied U-Pb systematics of zircon from pegmatites from the Finero complex, which is located at the Swiss/Italian border. These are alkaline pegmatites emplaced into mafic-ultramafic rocks. The host rocks were estimated to reside at temperatures in excess of 600 °C near the time of emplacement.

Zircon from these pegmatites forms crystals reaching 9 cm in length. The most studied crystal had an oscillatory-zoned rim of 200 µm width and a patchy core (Figure 1a,b). Its U-Pb analysis by in situ LA-ICP-MS yielded younger $^{206}\text{Pb}/^{238}\text{U}$ dates for the rim than for the core: two analyses from the rim were near 197 Ma (with a typical 2σ error of ± 2.5 Ma), while the analyses from the core had a weighted mean of 202.54 ± 0.46 Ma (2σ) and reached 205.7 Ma. TIMS U-Pb analysis of fragments from the same crystal yielded $^{206}\text{Pb}/^{238}\text{U}$ dates

that ranged from 200.7 ± 0.24 Ma (2σ) for its outer parts to 205.1 ± 0.22 Ma (2σ) for its core (Figure 1c,d). These variations were shown to correlate with zircon chemistry (Th-U-Ree contents and Nb/Ta and Th/U ratios) and Hf isotope systematics. Schaltegger et al. conclude that it took several growth episodes distributed over 4.5 Ma to form this crystal.

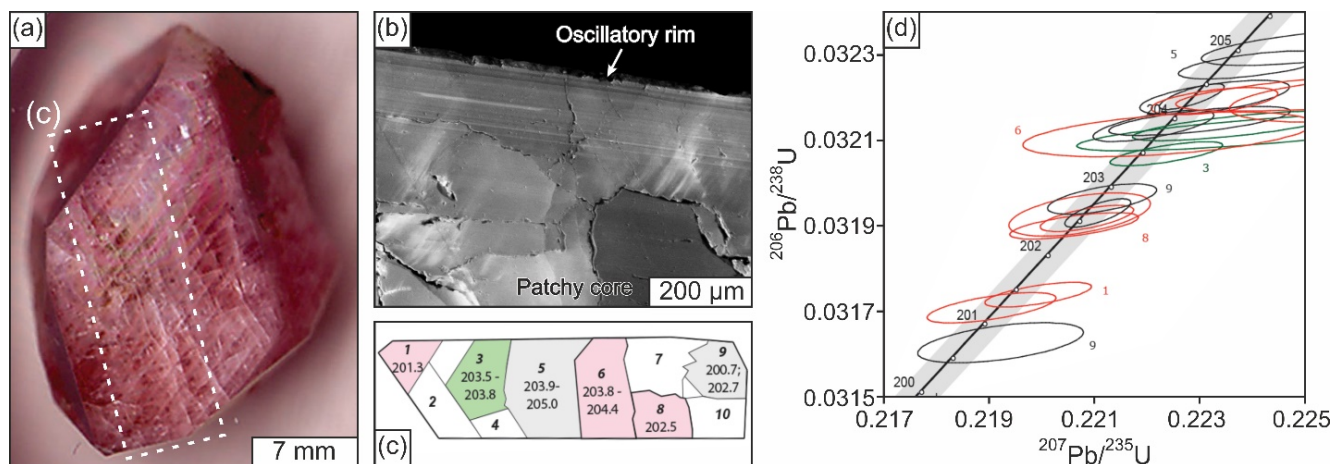


Figure 1. The results of U-Pb dating of zircon from pegmatites from the Finero complex (Swiss/Italian border) by Schaltegger et al. [30] (reproduced with permission from the Mineralogical Society of America). (a) Photograph of the most studied zircon crystal. (b) CL image of the outermost part of the crystal in (a). (c) Sketch showing the spatial distribution of the TIMS U-Pb dates obtained from the piece that was cut from the same crystal as shown in (a). (d) Concordia plot with all of the TIMS U-Pb data reported for the same crystal. Note the systematic rim-to-core increase in U-Pb dates that amounts to ~4.5 Ma.

2.2. Itrongay Pegmatite

Popov et al. [31] investigated the internal constitution and $^{40}\text{Ar}/^{39}\text{Ar}$ systematics of a gem-quality alkali feldspar crystal associated with pegmatites from the Itrongay locality in Madagascar. The crystal was picked from the ground near several pits with predominantly quartzofeldspathic pegmatites, which were emplaced while their host rocks cooled after a high-grade metamorphic event. The exact relationships between the crystal and the pegmatites are therefore unknown, although most previous studies regarded similar alkali feldspar from Itrongay as a pegmatitic phase [37–41].

CL and BSE imaging revealed five distinct zones in the alkali feldspar crystal, the first three of which were perfectly transparent and optically continuous, while the latter two represented optically discontinuous turbid surface coatings (Figure 2a–c) [31]. It was inferred that the first three zones formed from similar collections of substances, each including a silica gel and a CO_2 -rich fluid, while the latter two zones formed from an H_2O -dominated fluid. Initially, Popov et al. suggested that every zone formed well after the pegmatites in the area completed their crystallisation [31]. However, they later observed an analogous assemblage of inclusions comprising a silica gel and a CO_2 -rich fluid in a pegmatite sample, implying that the first three zones of the dated crystal and the pegmatites could have formed concurrently and are indeed genetically related to each other [8]. The turbid coatings can still be interpreted as some late alteration caused by an inflow of an H_2O -rich fluid having no connection to the pegmatite-forming process.

$^{40}\text{Ar}/^{39}\text{Ar}$ dates from within each zone of the alkali feldspar crystal were overdispersed; however, on average, each more exterior zone yielded younger $^{40}\text{Ar}/^{39}\text{Ar}$ dates than the preceding one (Figure 2d,e) [31]. Popov et al. showed that only the central part of the crystal may have partially lost ^{40}Ar by diffusion into hypothetical unevenly distributed inclusions, which may have caused the excess scatter of its $^{40}\text{Ar}/^{39}\text{Ar}$ dates around the mean value of 454 Ma. They therefore suggested that its age may rather be approximated by the K-Ca date of 477 ± 2 Ma (2σ) that was obtained for another similar crystal from

Itrongay by Nägler and Villa [38]. The overdispersion of $^{40}\text{Ar}/^{39}\text{Ar}$ dates in the following three zones (the outermost rim was not analysed) was explained by the presence of excess ^{40}Ar , so their ages were estimated as the mean of the second to fourth youngest analyses as, moving outwards, 401.7 ± 4.8 , 375.3 ± 4.5 and 176 ± 19 Ma (2σ). The gem-quality part of the crystal thus formed in three episodes distributed over ~ 100 Ma.

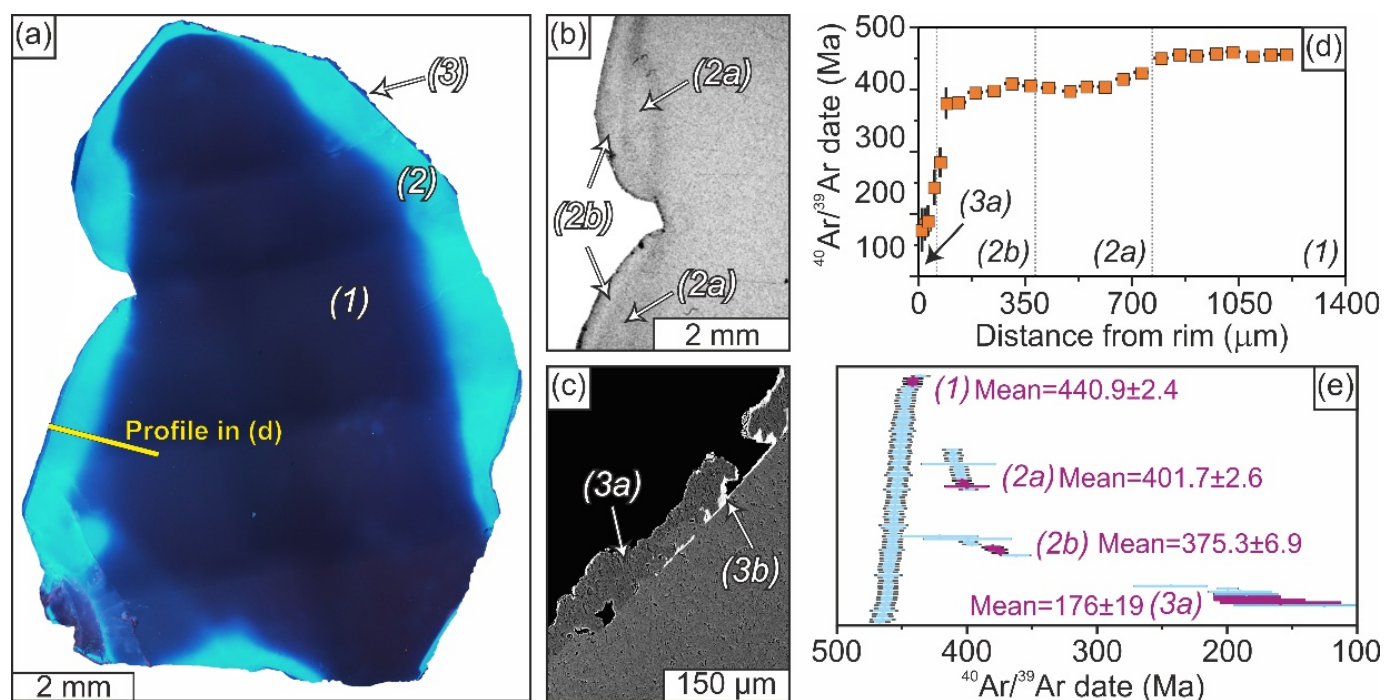


Figure 2. The results of Popov et al. [31] on in situ $^{40}\text{Ar}/^{39}\text{Ar}$ dating of a gem-quality crystal of alkali feldspar associated with the Itrongay pegmatites (Madagascar). (a) CL image of the dated crystal showing three major zones, which were produced in separate crystallisation events separated by dissolution events. (b–c) BSE images showing that each of the outer two zones can be further subdivided into two subzones, each reflecting a new growth event preceded by a dissolution event. (d) Rim-to-core in situ $^{40}\text{Ar}/^{39}\text{Ar}$ date profile that was acquired along the line shown in (a) and captured four inner (sub)zones that were wide enough to be analysed. (e) All of the in situ $^{40}\text{Ar}/^{39}\text{Ar}$ dates. Note that the in situ $^{40}\text{Ar}/^{39}\text{Ar}$ dates systematically increase towards the core of the crystal, including a ~ 200 Ma increase between turbid zone 3a and gem-quality zone 2b and a further ~ 100 Ma increase through gem-quality zones 2b, 2a and 1.

2.3. Pakeagama Lake Pegmatite

Smith et al. [28,29] published two studies of the Pakeagama Lake pegmatite from the Superior Province in Canada. This is a rare-element granitic pegmatite with beryl, petalite, spodumene, Li-rich mica, tourmaline and CGMs that forms a post-collisional intrusion in a greenstone belt with the exposure dimensions of 50 by 250 m. It was cut by veins that consist of quartz, Li-rich mica and CGMs, which were interpreted as the latest stage of crystallisation from a melt and a F-rich fluid.

The earlier study focussed on U-Pb geochronology of CGMs [28]. BSE images showed that CGMs have oscillatory zoning. In situ LA-ICP-MS U-Pb analysis of CGMs from the primary assemblage yielded $^{207}\text{Pb}/^{206}\text{Pb}$ dates that overlapped within 2σ uncertainties and had a weighted mean of 2670 ± 5 Ma (2σ). This value was interpreted as the age of initial emplacement. CGMs from the veins were analysed by in situ LA-ICP-MS and TIMS. The former method produced relatively imprecise $^{207}\text{Pb}/^{206}\text{Pb}$ dates that overlapped within 2σ uncertainties and had a weighted mean of 2661 ± 4 Ma (2σ), while the latter one yielded scattered $^{207}\text{Pb}/^{206}\text{Pb}$ dates ranging from 2638 ± 1 Ma to 2659 ± 1 Ma (2σ). The scatter was attributed to isotopic disturbances by later fluids. Note that this is a commonly invoked

process to explain scattered U-Pb dates from pegmatites, whether with or without support from petrological evidence [9–12,23–25].

The later study carried out in situ $^{40}\text{Ar}/^{39}\text{Ar}$ dating of mica from the primary assemblage [29]. BSE imaging revealed that the original muscovite is often replaced by mica with elevated measured F, Rb and Cs and inferred Li content along the edges of crystals and as veins across their cores (Figure 3a). Mica from the least altered sample yielded relatively uniform $^{40}\text{Ar}/^{39}\text{Ar}$ dates that range from 2625 ± 32 to 2674 ± 28 Ma (2σ), while mica from more altered samples yielded $^{40}\text{Ar}/^{39}\text{Ar}$ dates spanning from 2117 ± 22 to 2870 ± 32 Ma (2σ). This overall correlation between the presence of young $^{40}\text{Ar}/^{39}\text{Ar}$ dates and the degree of mica alteration sometimes manifested itself within individual $^{40}\text{Ar}/^{39}\text{Ar}$ date profiles, and altered domains yielded systematically younger $^{40}\text{Ar}/^{39}\text{Ar}$ dates than fresher ones in some crystals (Figure 3), although not in all of them. Smith et al. interpreted the formation of F-, Rb-, Cs- and Li-rich zones in mica as the integral part of the pegmatite formation process. This led them to attribute the observed $^{40}\text{Ar}/^{39}\text{Ar}$ date variations to diffusive loss of ^{40}Ar and hypothesise that the observed correlation of $^{40}\text{Ar}/^{39}\text{Ar}$ dates with composition is caused by related variations in mica's diffusion properties.

Although Smith et al. did raise the possibility that the $^{40}\text{Ar}/^{39}\text{Ar}$ date variations were created by fluid-induced dissolution–reprecipitation, they dismissed it because of the assumption that zoning in mica has fully developed within the timeframe of the fast pegmatite-forming process. However, without this assumption, their preferred interpretation becomes questionable, especially in the light of more recent research into the mechanisms of ^{40}Ar migration in micas, albeit mostly in muscovite. A growing number of studies have shown by combining in situ $^{40}\text{Ar}/^{39}\text{Ar}$ dating with petrological characterisation and occasionally Rb-Sr dating that fluid-mediated recrystallisation dominates ^{40}Ar redistribution in muscovite [42–44]. Furthermore, it has been recently demonstrated by atomistic simulations that ^{40}Ar diffusion in muscovite should be orders of magnitude slower than was previously inferred from in vacuo outgassing experiments, which renders the observation of ^{40}Ar concentration gradients formed by this process unlikely [45]. Therefore, I think that the possibility that the F-, Rb-, Cs- and Li-rich zones in mica are younger is viable.

For the sake of argument, I suggest an alternative explanation to the observations of Smith et al., which invokes two major crystallisation events in the history of the Pakeagama Lake pegmatite. The first one produced a rock with barren muscovite, and its age is captured by the $^{207}\text{Pb}/^{206}\text{Pb}$ dates of CGMs from the primary assemblage and amounts to 2670 ± 5 Ma (2σ). That rock could have had F, Rb, Cs and Li in it stored in some soluble form: combine the idea of Roedder [46] that miarolitic cavities are essentially large fluid inclusions with the observation of ramanite— $(\text{Cs,Rb})\text{B}_5\text{O}_8 \cdot 4\text{H}_2\text{O}$ —as a daughter phase in fluid inclusions *sensu strictiore* in minerals from pegmatites [47]. The second event caused the recrystallisation of muscovite that enriched it with F, Rb, Cs and Li in affected regions and the formation of veins with lepidolite, quartz and CGM crystals, the latter of which were inherited from the first stage. It is difficult to pin the age of this second event because of the scatter in $^{40}\text{Ar}/^{39}\text{Ar}$ dates. If the scatter results from the presence of excess ^{40}Ar , and the observation of $^{40}\text{Ar}/^{39}\text{Ar}$ dates exceeding the age of the first event suggest that it does, then the age of the second event would be best approximated by the youngest $^{40}\text{Ar}/^{39}\text{Ar}$ date of 2117 ± 22 Ma (2σ). The scatter of $^{207}\text{Pb}/^{206}\text{Pb}$ dates of CGMs could be related to partial resetting via fluid-mediated recrystallisation, as suggested by Smith et al.

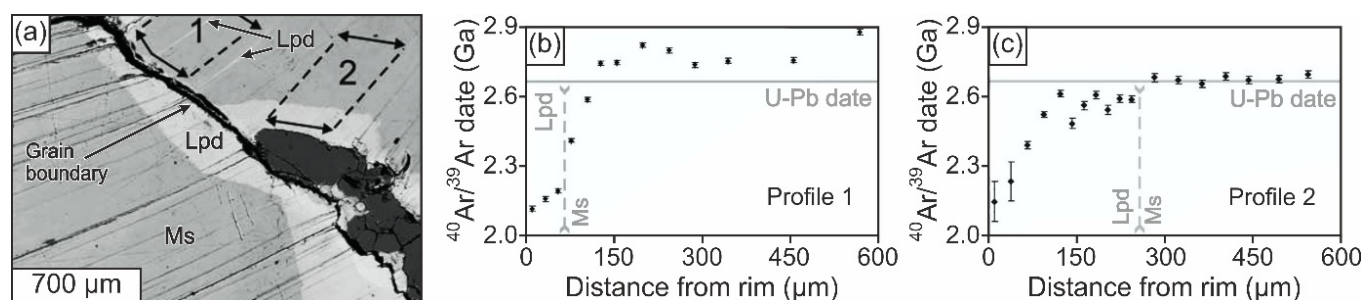


Figure 3. The results of in situ $^{40}\text{Ar}/^{39}\text{Ar}$ dating of mica from the Pakeagama Lake pegmatite (Canada) by Smith et al. [29] (reproduced with permission from Springer Nature). (a) BSE image showing two adjacent muscovite crystals that are replaced by F-, Rb-, Cs- and Li-rich mica along the boundary and occasionally along the cleavage. (b,c) Rim-to-core in situ $^{40}\text{Ar}/^{39}\text{Ar}$ date profiles obtained from the indicated regions within one of the crystals in (a). The horizontal lines in (b,c) show the average U-Pb date of CGM from the main pegmatite assemblage reported in the earlier work of Smith et al. [28]. Smith et al. [29] argued that $^{40}\text{Ar}/^{39}\text{Ar}$ dates falling above such line in (b) are so old because of the excess ^{40}Ar , which was introduced by the alteration along the cleavage that is visible in (a). Note that the F-, Rb-, Cs- and Li-rich mica yields generally younger dates than pristine muscovite.

2.4. Volyn Pegmatites

Franz et al. [32,48,49] researched how and when organic matter was brought to one of the Volyn rare-element pegmatites that are hosted by the Korosten granitic pluton in Ukraine. According to independent U-Pb dating of zircon and baddeleyite [50,51], the pluton was assembled between 1817 ± 15 and 1743 ± 5 Ma (the level of uncertainty was not indicated in the original sources). Zircon from pegmatites yielded upper concordia intercept dates between 1754 ± 4 and 1760 ± 3 Ma. Notably, the discordia fits were not always perfect (MSWD values reached 15), while this zircon had a similar appearance to that from the host rocks. Lower concordia intercepts for zircon from both pegmatites and their host rocks ranged from 0 to 550 Ma.

The initial study of Franz et al. [48] focussed on a pseudomorph after beryl, which was derived from a sample of breccia. The breccia was predominantly composed of clasts of feldspars and quartz in opaline cement. The pseudomorph itself consisted of opal, bertrandite, muscovite with tobelite overgrowths and buddingtonite (Figure 4a–c). It further contained some organic matter with cracks that were occasionally filled with opal. Franz et al. concluded that the pseudomorph formed in two stages, including (i) the replacement of beryl with muscovite and bertrandite and (ii) further alteration in the presence of organic matter that produced buddingtonite, tobelite and opal. The latter stage was suggested to have happened as soon as the Korosten intrusion cooled to sufficiently low temperatures to allow the existence of microbial life in it. The organic matter was thus suggested to be nearly as old as the Korosten intrusion, i.e., Paleoproterozoic.

The second study of Franz et al. [32] was based on the same pseudomorph and sought to verify the claim about the Precambrian age of the organic matter within it by $^{40}\text{Ar}/^{39}\text{Ar}$ dating of muscovite and buddingtonite. In contrast to the earlier paper, they asserted there that all of the minerals in the pseudomorph formed simultaneously, which was supported by the image from Figure 4b, where muscovite sheets supposedly “partly enclose buddingtonite”. The $^{40}\text{Ar}/^{39}\text{Ar}$ dates of muscovite ranged from 1439 ± 44 to 1545 ± 56 Ma (2σ), while those from buddingtonite span from 383 ± 24 to 563 ± 28 Ma (2σ). Franz et al. interpreted the muscovite dates as the age of the hydrothermal event that formed the pseudomorph and consequently as the age of the organic matter, while the buddingtonite dates were suggested to have been reset by the diffusive loss of ^{40}Ar .

The latest study of Franz et al. [49] was fully focussed on the organic matter and included an attempt to directly determine its age by U-Th-Pb analysis. They tried to analyse the organic matter from the pseudomorph; however, this did not yield meaningful

results: $^{238}\text{U}/^{206}\text{Pb}$ ratios, for example, ranged from 0.05 to 134 and showed no discernible correlation with $^{207}\text{Pb}/^{206}\text{Pb}$ ratios. Somewhat better results were obtained by analysing larger chunks of organic matter, most of which were taken from the cavity of one pegmatite: these yielded a statistically acceptable Pb-Pb isochron of 493 ± 196 Ma (2σ). Franz et al. reiterated their conclusion that the organic matter is Precambrian and at least as old as the oldest date of buddingtonite of 563 ± 28 Ma (2σ).

Clearly, $^{40}\text{Ar}/^{39}\text{Ar}$ results prompted Franz et al. to change their views on the timing of the pseudomorph formation. While they initially regarded the replacement of beryl as the integral part of the sequence of processes that produced the Volyn pegmatites near ~1760 Ma, they later ascribed it to an independent hydrothermal event near ~1440 Ma. This change of mind on its own is very illustrative in the context of my paper. However, in my opinion, their data suggest an even more protracted history of interaction with fluids. As detailed below, I think the presented evidence suggests that the assemblage of buddingtonite, tobelite, opal and organic matter could well be Phanerozoic in age.

Firstly, BSE images published by Franz et al. show that buddingtonite is associated with tobelite and opal. This assemblage of minerals often occurs in patches and veins with sharp compositional boundaries, which are clearly discernible even when tobelite forms epitaxial overgrowths on muscovite (Figure 4c). Such textures are typically produced by fluid-mediated replacement [52], and thus I can only concur with the initial interpretation of Franz et al. that the assemblage with buddingtonite overprinted the assemblage with muscovite. Their later argument that the two assemblages were contemporary because muscovite sheets in Figure 4b embrace buddingtonite seems weak to me. Buddingtonite in this BSE image displays concentric zoning around nucleation points on or near the surfaces of muscovite and includes deformed and broken muscovite sheets, which rather indicates that it grew on and within splintered muscovite.

Secondly, there is presently no unambiguous evidence to substantiate the claim of Franz et al. that the $^{40}\text{Ar}/^{39}\text{Ar}$ dates of buddingtonite are younger than those of muscovite because of diffusive loss of ^{40}Ar . Although the mechanisms of ^{40}Ar redistribution in buddingtonite have not been studied, there is a lot of relevant work on alkali feldspar, which combined $^{40}\text{Ar}/^{39}\text{Ar}$ analysis with petrological characterisation to show that fluid-mediated recrystallisation is the dominant one [42,53], including in the case of the Itrongay feldspar (see above), which used to serve as the most convincing example of alkali feldspar that lost ^{40}Ar by diffusion [41]. Franz et al. suggested that the presence of grain boundaries would somehow facilitate diffusive loss of ^{40}Ar ; however, both $^{40}\text{Ar}/^{39}\text{Ar}$ dating of polycrystalline authigenic feldspar [54] and experiments on ^{40}Ar diffusion in recrystallised feldspar [55] question the efficiency of grain boundaries as fast pathways for ^{40}Ar loss. Therefore, it is likely that buddingtonite yielded younger $^{40}\text{Ar}/^{39}\text{Ar}$ dates than muscovite because it is indeed younger.

Thus, in my opinion, both petrological and geochronological evidence indicate that the Volyn pegmatites have experienced at least two major fluid interaction events after the initial emplacement, one that formed the beryl-replacing assemblage with muscovite and another that produced the beryl-replacing assemblage with buddingtonite. The precise timeframes of these events are difficult to establish. The spread in $^{40}\text{Ar}/^{39}\text{Ar}$ dates indicates that both could be protracted; however, it could also result from the presence of excess ^{40}Ar . The latter seems to account for some of the $^{40}\text{Ar}/^{39}\text{Ar}$ date variation in the Itrongay feldspar and Pakeagama Lake mica (see above), as well as in micas and feldspars that grew in metamorphic environments [56,57], including by fluid-induced dissolution-precipitation [57]. Regardless, the data as they stand suggest that the first fluid interaction event was Proterozoic, while the second one was Phanerozoic. The Phanerozoic age of the buddingtonite-forming event is corroborated by the Pb-Pb isochron of 493 ± 196 Ma (2σ) defined by the analyses of organic matter and the lower concordia intercepts of 0 to 550 Ma defined by the analyses of zircon.

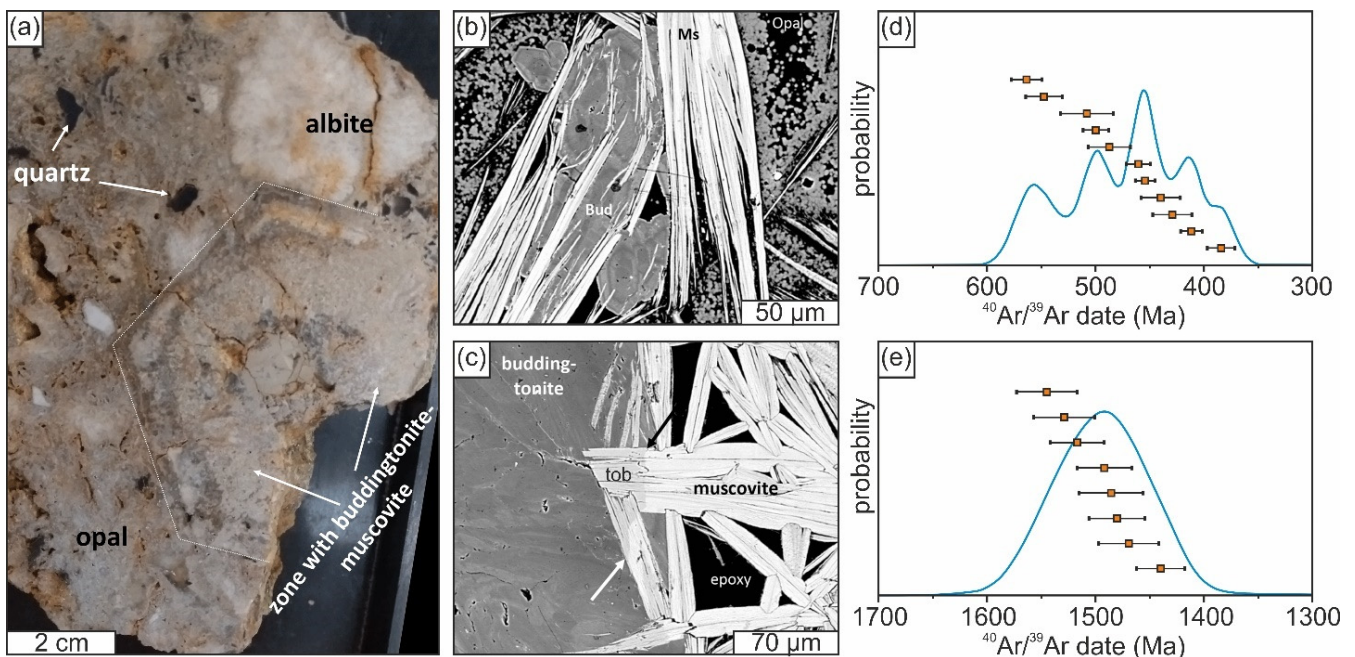


Figure 4. The results of Franz et al. [32] on in situ $^{40}\text{Ar}/^{39}\text{Ar}$ dating of muscovite and buddingtonite from a pseudomorph after beryl from one of the Volyn pegmatites (Ukraine). (a) Overview photograph of the sample with the studied pseudomorph. (b,c) BSE images showing the relationships between muscovite, buddingtonite, tobelite and opal within the pseudomorph. (d,e) Plots with individual in situ $^{40}\text{Ar}/^{39}\text{Ar}$ dates and probability density functions built from them for buddingtonite (d) and muscovite (e). Note that buddingtonite yielded significantly younger $^{40}\text{Ar}/^{39}\text{Ar}$ dates than muscovite and that there is a considerable scatter in each set of $^{40}\text{Ar}/^{39}\text{Ar}$ dates.

3. Discussion

The idea that pegmatite crystallisation is a fast process follows from the calculated cooling rates for the pegmatites of the San Diego County in California, USA [15–17]. These calculations assumed that 1 to 25 m thick dykes had the initial temperature of $\sim 650\text{ }^{\circ}\text{C}$, were hosted by rocks with the temperature of $\sim 150\text{ }^{\circ}\text{C}$ and cooled by conductive heat transfer. The results show that the central part of the thinnest of the dykes cooled below $550\text{ }^{\circ}\text{C}$ in just ~ 5 days, while the thickest one cooled to the same temperature in ~ 9 years. If it is further assumed that $550\text{ }^{\circ}\text{C}$ was the solidus temperature and thus crystallisation was complete upon reaching it, as was assumed in the cited works, then a conclusion can be drawn that these pegmatites crystallised rapidly, in ~ 5 days to ~ 9 years. However, it is unclear how valid the latter assumption is, considering that pegmatites may crystallise from undercooled melts [1] or even gels [7,8], which potentially can happen after cooling to the country rock temperature and last for a while [8,58]. Furthermore, the conclusion that follows from this assumption itself raises some questions. Why do pegmatites of different thickness display similar textures? In other words, why are these textures insensitive to the cooling rate? And why do pegmatites that are hosted within or near their parent granites and thus must have cooled much more slowly often display similar textures?

Notwithstanding, the idea that pegmatites crystallise rapidly became very popular in recent years and had an underpinning role in how these rocks were thought about. Very illustrative of that and at the same time pertinent to the present discussion is the study of Phelps et al. [59], who modelled trace element profiles in quartz from one of the pegmatites of the San Diego County to suggest that it grew in just a few hours (Figure 5). Their modelling utilised equations derived to predict chemical gradients in certain artificial systems for crystal synthesis [60,61], so the application of these equations to a natural environment seems questionable. For example, Phelps et al. infer that the flow of fluid around the quartz crystal was turbulent, and I do not see how this inference can be

reconciled with their modelling approach, which assumed that fluid did not flow, not even with the help of their response to the same criticism from Reviewer #3 of their manuscript that was published alongside. However, I think that the importance of such details dims when the CL image of their quartz crystal (Figure 5a) is simply compared with the CL image of the aforementioned alkali feldspar crystal from the Itrongay feldspar (Figure 2a). As indicated in Andrea Dini's review of Phelps et al., which was also published alongside their manuscript, this quartz crystal clearly had a complex history. How can we be sure that it did not last for millions of years?

Of course, having only four isolated and potentially controversial examples of protracted mineral growth in pegmatites is not enough to defend the point that the formation of these rocks is always a protracted, multi-stage process. The example of the Finero pegmatite may be deemed exotic and not representative of pegmatites that are referred to as granitic, while the other three examples may be taken as characterising some late-stage processes in specific bodies that are not relevant to the pegmatite-forming process in general. However, there are not so many other studies providing geochronological data with a comparable level of petrological support to demonstrate the trivial nature of these four examples, while the available evidence for rapid crystallisation of pegmatites is imperfect. Therefore, I think that the data reviewed here do warrant a more systematic and model-independent look into the timescales of mineral growth in pegmatites. Whether it turns out that pegmatites form slowly as a whole or that only some minerals in them tend to considerably postdate the initial emplacement, such work can provide one of the keys to fully understand how these rocks form.

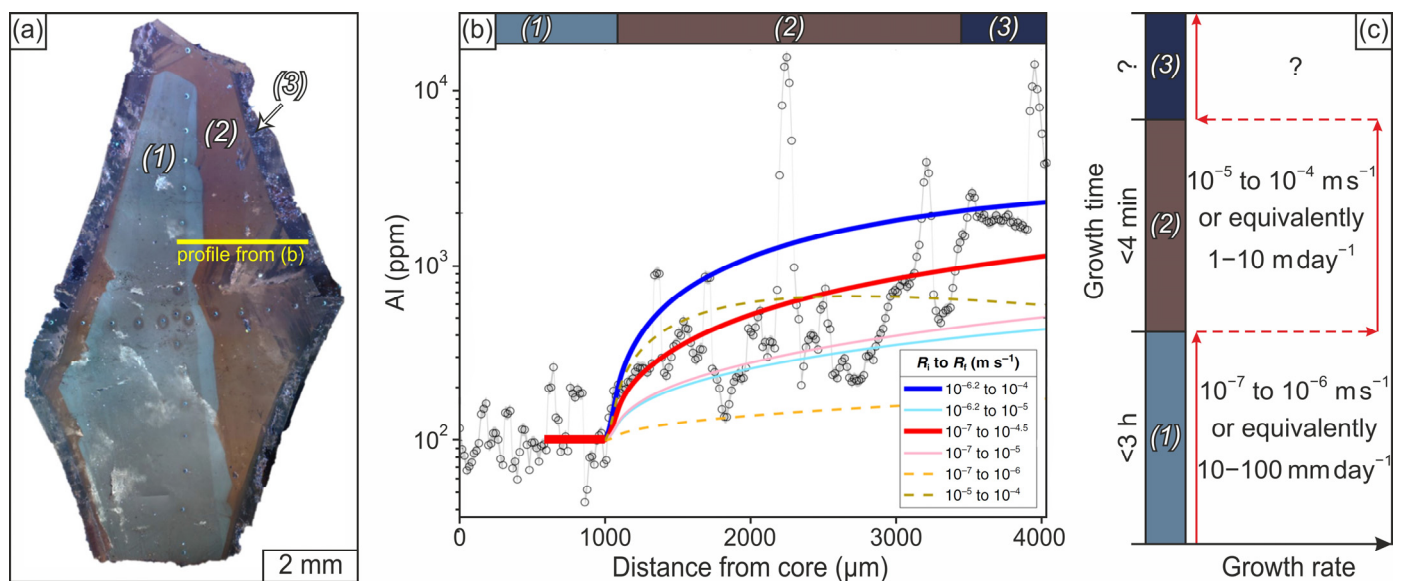


Figure 5. The estimates of Phelps et al. [59] for the growth rates of a quartz crystal from a pegmatite from the San Diego County (CA, USA) with some of the underlying data. (a) CL image of the quartz crystal. (b) Core-to-rim Al concentration profile from the crystal in (a) that was modelled to constrain the growth rates of its zones 1 and 2. Coloured lines show modelling outcomes for different assumed growth rates (R_i to R_f) at the start and the end of the crystallisation of zone 2. (c) Reconstructed growth history for the same crystal. Note the similarity between the CL images of this quartz crystal and the crystal of alkali feldspar from Figure 2.

4. Conclusions

Recent research on pegmatites converges on the idea that they crystallise rapidly, with some estimates of crystal growth rates reaching a staggering 10 m/day [59]. However, several studies that present geochronological data backed by petrological characterisation provide grounds to question this idea and sketch a wholly different picture of protracted and potentially polygenic mineral growth in pegmatites. Although these studies are clearly

insufficient to make firm generalised conclusions, they indicate that the timescales over which individual pegmatites form should be investigated further and highlight that isotopic dating is viable tool for doing so.

Funding: This research received no external funding.

Institutional Review Board Statement: Not applicable.

Informed Consent Statement: Not applicable.

Data Availability Statement: No original data presented.

Acknowledgments: I am grateful to Tumyshev's family, who helped me an awful lot over the past months, so that I have found energy and motivation to work on this manuscript. The editorial office of Geosciences is thanked for their invitation to prepare a feature paper, which resulted in this contribution. I further thank F. Guo for the editorial handling and M. Z. El-Bialy and two anonymous reviewers for their comments, which helped to improve my manuscript.

Conflicts of Interest: The author declares no conflict of interest. No funders had any role in the design of the study; in the collection, analysis, or interpretation of data; in the writing of the manuscript; or in the decision to publish the results.

References

1. London, D. A Petrologic Assessment of Internal Zonation in Granitic Pegmatites. *Lithos* **2014**, *184–187*, 74–104. [[CrossRef](#)]
2. Simmons, W.B.; Pezzotta, F.; Shigley, J.E.; Beurlen, H. Granitic Pegmatites as Sources of Colored Gemstones. *Elements* **2012**, *8*, 281–287. [[CrossRef](#)]
3. Glover, A.S.; Rogers, W.Z.; Barton, J.E. Granitic Pegmatites: Storehouses of Industrial Minerals. *Elements* **2012**, *8*, 269–273. [[CrossRef](#)]
4. Linnen, R.L.; Van Lichtenvelde, M.; Černý, P. Granitic Pegmatites as Sources of Strategic Metals. *Elements* **2012**, *8*, 275–280. [[CrossRef](#)]
5. Troch, J.; Huber, C.; Bachmann, O. The Physical and Chemical Evolution of Magmatic Fluids in Near-Solidus Silicic Magma Reservoirs: Implications for the Formation of Pegmatites. *Am. Mineral.* **2022**, *107*, 190–205. [[CrossRef](#)]
6. Thomas, R.; Davidson, P. Comment on “A Petrologic Assessment of Internal Zonation in Granitic Pegmatites” by David London (2014). *Lithos* **2015**, *212–215*, 462–468. [[CrossRef](#)]
7. Smirnov, S.Z. The Fluid Regime of Crystallization of Water-Saturated Granitic and Pegmatitic Magmas: A Physicochemical Analysis. *Russ. Geol. Geophys.* **2015**, *56*, 1292–1307. [[CrossRef](#)]
8. Popov, D.V.; Spikings, R.A.; Razakamanana, T. Inclusions of Amorphous and Crystalline SiO₂ in Minerals from Itrongay (Madagascar) and Other Evidence for the Natural Occurrence of Hydrosilicate Fluids. *Geosciences* **2022**, *12*, 28. [[CrossRef](#)]
9. Romer, R.L.; Smeds, S.-A. U-Pb Columbite Chronology of Post-Kinematic Palaeoproterozoic Pegmatites in Sweden. *Precambrian Res.* **1997**, *82*, 85–99. [[CrossRef](#)]
10. Müller, A.; Romer, R.L.; Pedersen, R.-B. The Sveconorwegian Pegmatite Province—Thousands of Pegmatites Without Parental Granites. *Can. Mineral.* **2017**, *55*, 283–315. [[CrossRef](#)]
11. Kontak, D.J.; Creaser, R.A.; Heaman, L.M.; Archibald, D.A. U-Pb Tantalite, Re-Os Molybdenite, and ⁴⁰Ar/³⁹Ar Muscovite Dating of the Brazil Lake Pegmatite, Nova Scotia: A Possible Shear-Zone Related Origin for an LCT-Type Pegmatite. *Atl. Geol.* **2005**, *41*, 17–29. [[CrossRef](#)] [[PubMed](#)]
12. Shaw, R.A.; Goodenough, K.M.; Roberts, N.M.W.; Horstwood, M.S.A.; Chenery, S.R.; Gunn, A.G. Petrogenesis of Rare-Metal Pegmatites in High-Grade Metamorphic Terranes: A Case Study from the Lewisian Gneiss Complex of North-West Scotland. *Precambrian Res.* **2016**, *281*, 338–362. [[CrossRef](#)]
13. Melleton, J.; Gloaguen, E.; Frei, D.; Novak, M.; Breiter, K. How Are the Emplacement of Rare-Element Pegmatites, Regional Metamorphism and Magmatism Interrelated in the Moldanubian Domain of the Variscan Bohemian Massif, Czech Republic? *Can. Mineral.* **2012**, *50*, 1751–1773. [[CrossRef](#)]
14. Lv, Z.-H.; Zhang, H.; Tang, Y. Anatexis Origin of Rare Metal/Earth Pegmatites: Evidences from the Permian Pegmatites in the Chinese Altai. *Lithos* **2021**, *380–381*, 105865. [[CrossRef](#)]
15. Simmons, W.B.; Webber, K.L. Pegmatite Genesis: State of the Art. *Eur. J. Mineral.* **2008**, *20*, 421–438. [[CrossRef](#)]
16. Webber, K.L.; Simmons, W.B.; Falster, A.U.; Foord, E.E. Cooling Rates and Crystallization Dynamics of Shallow Level Pegmatite-Aplite Dikes, San Diego County, California. *Am. Mineral.* **1999**, *84*, 708–717. [[CrossRef](#)]
17. Webber, K.L.; Falster, A.U.; Simmons, W.B.; Foord, E.E. The Role of Diffusion-Controlled Oscillatory Nucleation in the Formation of Line Rock in Pegmatite-Plite Dikes. *J. Petrol.* **1997**, *38*, 1777–1791. [[CrossRef](#)]
18. Bradley, D.; Shea, E.; Buchwaldt, R.; Bowring, S.; Benowitz, J.; O'Sullivan, P.; McCauley, A. Geochronology and Tectonic Context of Lithium-Cesium-Tantalum Pegmatites In the Appalachians. *Can. Mineral.* **2016**, *54*, 945–969. [[CrossRef](#)]

19. Mauthner, M.H.F.; Mortensen, J.K.; Groat, L.A.; Ercit, T.S. Geochronology of the Little Nahanni Pegmatite Group, Selwyn Mountains, Southwestern Northwest Territories. *Can. J. Earth Sci.* **1995**, *32*, 2090–2097. [[CrossRef](#)]
20. McCauley, A.; Bradley, D.C. The Global Age Distribution of Granitic Pegmatites. *Can. Mineral.* **2014**, *52*, 183–190. [[CrossRef](#)]
21. Melcher, F.; Graupner, T.; Gäbler, H.-E.; Sitnikova, M.; Henjes-Kunst, F.; Oberthür, T.; Gerdes, A.; Dewaele, S. Tantalum–(Niobium–Tin) Mineralisation in African Pegmatites and Rare Metal Granites: Constraints from Ta–Nb Oxide Mineralogy, Geochemistry and U–Pb Geochronology. *Ore Geol. Rev.* **2015**, *64*, 667–719. [[CrossRef](#)]
22. Tkachev, A.V. Evolution of Metallogeny of Granitic Pegmatites Associated with Orogens throughout Geological Time. *Geol. Soc. Lond. Spec. Publ.* **2011**, *350*, 7–23. [[CrossRef](#)]
23. Wang, H.-Y.; Tang, Y.; Zhang, H.; Lv, Z.-H.; Xu, Y.-S. The Geochronology of the Rare Metal Pegmatite Deposits: A Case Study in Nanping No. 31 Pegmatite Vein in Northeastern Cathaysian Block, China. *Ore Geol. Rev.* **2023**, *153*, 105280. [[CrossRef](#)]
24. Sun, W.; Zhao, Z.; Mo, X.; Wei, C.; Dong, G.; Li, X.; Yuan, W.; Wang, T.; Yang, S.; Wang, B.; et al. Age and Composition of Columbite-Tantalite Group Minerals in the Spodumene Pegmatite from the Chakabeishan Deposit, Northern Tibetan Plateau and Their Implications. *Minerals* **2023**, *13*, 201. [[CrossRef](#)]
25. Konzett, J.; Schneider, T.; Nedyalkova, L.; Hauenberger, C.; Melcher, F.; Gerdes, A.; Whitehouse, M. Anatectic Granitic Pegmatites from the Eastern Alps: A Case of Variable Rare-Metal Enrichment During High-Grade Regional Metamorphism—I: Mineral Assemblages, Geochemical Characteristics, and Emplacement Ages. *Can. Mineral.* **2018**, *56*, 555–602. [[CrossRef](#)]
26. Bryden, C.D.; Jamieson, R.A.; Luo, Y.; Fisher, C.M.; Pearson, D.G. Geochronology of Scapolite Pegmatites from the Nordøyane Ultra-High-Pressure Domain, Western Gneiss Region, Norway: Protracted Crystal-Melt Reaction during Scandian Exhumation. *Lithos* **2022**, *424–425*, 106756. [[CrossRef](#)]
27. Feng, Y.; Jiang, S.-Y.; Wang, C.-L.; Jin, G.; Zhang, J.; Zhang, H.-X.; Hu, X.-J. U–Pb Geochronology of Columbite-Group Mineral, Cassiterite, and Zircon and Hf Isotopes for Devonian Rare-Metal Pegmatite in the Nanyangshan Deposit, North Qinling Orogenic Belt, China. *Ore Geol. Rev.* **2022**, *140*, 104634. [[CrossRef](#)]
28. Smith, S.R.; Foster, G.L.; Romer, R.L.; Tindle, A.G.; Kelley, S.P.; Noble, S.R.; Horstwood, M.; Breaks, F.W. U-Pb Columbite-Tantalite Chronology of Rare-Element Pegmatites Using TIMS and Laser Ablation-Multi Collector-ICP-MS. *Contrib. Mineral. Petrol.* **2004**, *147*, 549–564. [[CrossRef](#)]
29. Smith, S.R.; Kelley, S.P.; Tindle, A.G.; Breaks, F.W. Compositional Controls on $^{40}\text{Ar}/^{39}\text{Ar}$ Ages of Zoned Mica from a Rare-Element Pegmatite. *Contrib. Mineral. Petrol.* **2005**, *149*, 613–626. [[CrossRef](#)]
30. Schaltegger, U.; Ulianov, A.; Muntener, O.; Ovtcharova, M.; Peytcheva, I.; Vonlanthen, P.; Vennemann, T.; Antognini, M.; Girlanda, F. Megacrystic Zircon with Planar Fractures in Miaskite-Type Nepheline Pegmatites Formed at High Pressures in the Lower Crust (Ivrea Zone, Southern Alps, Switzerland). *Am. Mineral.* **2015**, *100*, 83–94. [[CrossRef](#)]
31. Popov, D.V.; Spikings, R.A.; Scaillet, S.; O’Sullivan, G.; Chew, D.; Badenszki, E.; Daly, J.S.; Razakamanana, T.; Davies, J.H.F.L. Diffusion and Fluid Interaction in Itrongay Pegmatite (Madagascar): Evidence from in Situ $^{40}\text{Ar}/^{39}\text{Ar}$ Dating of Gem-Quality Alkali Feldspar and U-Pb Dating of Protogenetic Apatite Inclusions. *Chem. Geol.* **2020**, *556*, 119841. [[CrossRef](#)]
32. Franz, G.; Sudo, M.; Khomenko, V. $^{40}\text{Ar}/^{39}\text{Ar}$ Dating of a Hydrothermal Pegmatitic Buddingtonite–Muscovite Assemblage from Volyn, Ukraine. *Eur. J. Mineral.* **2022**, *34*, 7–18. [[CrossRef](#)]
33. Naumenko-Dèzes, M.O.; Villa, I.M.; Rolland, Y.; Gallet, S.; Lanari, P. Subgrain $^{40}\text{Ar}/^{39}\text{Ar}$ Dating of Museum-Quality Micas Reveals Intragrain Heterogeneity. *Chem. Geol.* **2021**, *573*, 120215. [[CrossRef](#)]
34. Michallik, R.M.; Wagner, T.; Fusswinkel, T.; Heinonen, J.S.; Heikkilä, P. Chemical Evolution and Origin of the Luumäki Gem Beryl Pegmatite: Constraints from Mineral Trace Element Chemistry and Fractionation Modeling. *Lithos* **2017**, *274–275*, 147–168. [[CrossRef](#)]
35. Dill, H.G.; Skoda, R.; Weber, B.; Müller, A.; Berner, Z.A.; Wemmer, K.; Balaban, S.-I. Mineralogical and Chemical Composition of the Hagendorf-North Pegmatite, SE Germany—A Monographic Study. *Neues Jahrb. Für Mineral. Abh.* **2013**, *190*, 281–318. [[CrossRef](#)]
36. Zagorsky, V.Y. Sosedka Pegmatite Body at the Malkhan Deposit of Gem Tourmaline, Transbaikalia: Composition, Inner Structure, and Petrogenesis. *Petrology* **2015**, *23*, 68–92. [[CrossRef](#)]
37. Lacroix, A. Note Préliminaire Sur Quelques Minéraux de Madagascar Dont Plusieurs Peuvent Être Utilisés Comme Gemmes. *Comptes Rendus Hebd. Séances L’académie Sci.* **1912**, *155*, 672–677.
38. Nägler, T.F.; Villa, I.M. In Pursuit of the ^{40}K Branching Ratios: K–Ca and ^{39}Ar – ^{40}Ar Dating of Gem Silicates. *Chem. Geol.* **2000**, *169*, 5–16. [[CrossRef](#)]
39. Simmons, W.B.; Falster, A.U. Yellow Orthoclase (Sanidine) from South Betroka, Madagascar. *Mineral. Rec.* **2002**, *33*, 79–80.
40. Parsons, I.; Lee, M.R. Minerals Are Not Just Chemical Compounds. *Can. Mineral.* **2005**, *43*, 1959–1992. [[CrossRef](#)]
41. Flude, S.; Halton, A.M.; Kelley, S.P.; Sherlock, S.C.; Schwanethal, J.; Wilkinson, C.M. Observation of Centimetre-Scale Argon Diffusion in Alkali Feldspars: Implications for $^{40}\text{Ar}/^{39}\text{Ar}$ Thermochronology. *Geol. Soc. Lond. Spec. Publ.* **2014**, *378*, 265–275. [[CrossRef](#)]
42. Spikings, R.A.; Popov, D.V. Thermochronology of Alkali Feldspar and Muscovite at $T > 150\text{ }^\circ\text{C}$ Using the $^{40}\text{Ar}/^{39}\text{Ar}$ Method: A Review. *Minerals* **2021**, *11*, 1025. [[CrossRef](#)]
43. Halama, R.; Glodny, J.; Konrad-Schmolke, M.; Sudo, M. Rb–Sr and in Situ $^{40}\text{Ar}/^{39}\text{Ar}$ Dating of Exhumation-Related Shearing and Fluid-Induced Recrystallization in the Sesia Zone (Western Alps, Italy). *Geosphere* **2018**, *14*, 1425–1450. [[CrossRef](#)]

44. Villa, I.M.; Glodny, J.; Peillod, A.; Skelton, A.; Ring, U. Petrochronology of Polygenetic White Micas (Naxos, Greece). *J. Metamorph. Geol.* **2023**, *41*, 401–423. [[CrossRef](#)]
45. Nteme, J.; Scaillet, S.; Brault, P.; Tassan-Got, L. Atomistic Simulations of ^{40}Ar Diffusion in Muscovite. *Geochim. Cosmochim. Acta* **2022**, *331*, 123–142. [[CrossRef](#)]
46. Roedder, E. Fluid Inclusion Evidence for Immiscibility in Magmatic Differentiation. *Geochim. Cosmochim. Acta* **1992**, *56*, 5–20. [[CrossRef](#)]
47. Thomas, R.; Davidson, P.; Hahn, A. Ramanite-(Cs) and Ramanite-(Rb): New Cesium and Rubidium Pentaborate Tetrahydrate Minerals Identified with Raman Spectroscopy. *Am. Mineral.* **2008**, *93*, 1034–1042. [[CrossRef](#)]
48. Franz, G.; Khomenko, V.; Vishnyevskyy, A.; Wirth, R.; Struck, U.; Nissen, J.; Gernert, U.; Rocholl, A. Biologically Mediated Crystallization of Buddingtonite in the Paleoproterozoic: Organic-Igneous Interactions from the Volyn Pegmatite, Ukraine. *Am. Mineral.* **2017**, *102*, 2119–2135. [[CrossRef](#)]
49. Franz, G.; Lyckberg, P.; Khomenko, V.; Chournousenko, V.; Schulz, H.-M.; Mahlstedt, N.; Wirth, R.; Glodny, J.; Gernert, U.; Nissen, J. Fossilization of Precambrian Microfossils in the Volyn Pegmatite, Ukraine. *Biogeosciences* **2022**, *19*, 1795–1811. [[CrossRef](#)]
50. Shumlyanskyy, L.; Hawkesworth, C.; Billström, K.; Bogdanova, S.; Mytrokhyn, O.; Romer, R.; Dhuime, B.; Claesson, S.; Ernst, R.; Whitehouse, M.; et al. The Origin of the Palaeoproterozoic AMCG Complexes in the Ukrainian Shield: New U-Pb Ages and Hf Isotopes in Zircon. *Precambrian Res.* **2017**, *292*, 216–239. [[CrossRef](#)]
51. Shumlyanskyy, L.; Franz, G.; Glynn, S.; Mytrokhyn, O.; Voznyak, D.; Bilan, O. Geochronology of Granites of the Western Korosten AMCG Complex (Ukrainian Shield): Implications for the Emplacement History and Origin of Mirolitic Pegmatites. *Eur. J. Mineral.* **2021**, *33*, 703–716. [[CrossRef](#)]
52. Putnis, A. Mineral Replacement Reactions. *Rev. Mineral. Geochem.* **2009**, *70*, 87–124. [[CrossRef](#)]
53. Villa, I.M. Diffusion in Mineral Geochronometers: Present and Absent. *Chem. Geol.* **2016**, *420*, 1–10. [[CrossRef](#)]
54. Mark, D.F.; Kelley, S.P.; Lee, M.R.; Parnell, J.; Sherlock, S.C.; Brown, D.J. Ar–Ar Dating of Authigenic K-Feldspar: Quantitative Modelling of Radiogenic Argon-Loss through Subgrain Boundary Networks. *Geochim. Cosmochim. Acta* **2008**, *72*, 2695–2710. [[CrossRef](#)]
55. Popov, D.V.; Spikings, R.A.; Kouzmanov, K. Pathways for ^{39}Ar Loss during Step-Heating of Alkali Feldspar Megacrysts from the Shap Granite (UK): Combined Evidence from Diffusion Experiments and Characterisation of Heating-Induced Texture Modifications. *Chem. Geol.* **2020**, *547*, 119677. [[CrossRef](#)]
56. Scibiorski, E.; Jourdan, F.; Mezger, K.; Tohver, E.; Vollstaedt, H. Cryptic Excess Argon in Metamorphic Biotite: Anomalously Old $^{40}\text{Ar}/^{39}\text{Ar}$ Plateau Dates Tested with Rb/Sr Thermochronology and Ar Diffusion Modelling. *Geochim. Cosmochim. Acta* **2021**, *315*, 1–23. [[CrossRef](#)]
57. Popov, D.; Spikings, R.; Ovtcharova, M.; O’Sullivan, G.; Chew, D.; Badenszki, E.; Daly, S.; Davies, J.; Chiaradia, M.; Ulianov, A. Multi-Method Approach to Understanding the Migration Mechanisms of Pb in Apatite and Ar in Alkali Feldspar from Proterozoic Granitic Batholiths from the Mt. Isa Inlier (Australia). In Proceedings of the Goldschmidt Conference 2021, Virtual, 4–9 July 2021.
58. London, D. An Experimental Crystallization Of The Macusani Obsidian In A Thermal Gradient With Applications To Lithium-Rich Granitic Pegmatites. *Am. Mineral.* *in press*. [[CrossRef](#)]
59. Phelps, P.R.; Lee, C.-T.A.; Morton, D.M. Episodes of Fast Crystal Growth in Pegmatites. *Nat. Commun.* **2020**, *11*, 4986. [[CrossRef](#)]
60. Burton, J.A.; Prim, R.C.; Slichter, W.P. The Distribution of Solute in Crystals Grown from the Melt. *Part I. Theoretical*. *J. Chem. Phys.* **1953**, *21*, 1987–1991. [[CrossRef](#)]
61. Smith, V.G.; Tiller, W.A.; Rutter, J.W. A Mathematica Analysis of Solute Redistribution during Solidification. *Can. J. Phys.* **1955**, *33*, 723–745. [[CrossRef](#)]

Disclaimer/Publisher’s Note: The statements, opinions and data contained in all publications are solely those of the individual author(s) and contributor(s) and not of MDPI and/or the editor(s). MDPI and/or the editor(s) disclaim responsibility for any injury to people or property resulting from any ideas, methods, instructions or products referred to in the content.